

In vitro and *in vivo* evaluation of SLA titanium surfaces with further alkali or hydrogen peroxide and heat treatment

This article has been downloaded from IOPscience. Please scroll down to see the full text article.

2011 Biomed. Mater. 6 025001

(<http://iopscience.iop.org/1748-605X/6/2/025001>)

View [the table of contents for this issue](#), or go to the [journal homepage](#) for more

Download details:

IP Address: 162.105.195.240

The article was downloaded on 05/02/2011 at 01:39

Please note that [terms and conditions apply](#).

In vitro and *in vivo* evaluation of SLA titanium surfaces with further alkali or hydrogen peroxide and heat treatment

E W Zhang^{1,2}, Y B Wang^{1,2}, K G Shuai², F Gao², Y J Bai², Y Cheng², X L Xiong², Y F Zheng^{1,4} and S C Wei^{3,4}

¹ State Key Laboratory for Turbulence and Complex System, Department of Advanced Materials and Nanotechnology, College of Engineering, Peking University, Beijing 100871, People's Republic of China

² Center for Biomedical Materials and Tissue Engineering, Academy for Advanced Interdisciplinary Studies, Peking University, Beijing 100871, People's Republic of China

³ Department of Oral and Maxillofacial Surgery, School of Stomatology, Peking University, Beijing 100081, People's Republic of China

E-mail: enwei@pku.edu.cn, yanbo.pku@pku.edu.cn, shuaikegang@gmail.com, soarfgoal@gmail.com, norice86@163.com, chengyan@pku.edu.cn, xxiaoling11@hotmail.com, yfzheng@pku.edu.cn and weishicheng99@163.com

Received 10 August 2010

Accepted for publication 12 January 2011

Published 4 February 2011

Online at stacks.iop.org/BMM/6/025001

Abstract

The present study aimed to evaluate the bioactivity of titanium surfaces sandblasted with large-grit corundum and acid etched (SLA) plus further alkali or hydrogen peroxide and heat treatment for dental implant application. Pure titanium disks were mechanically polished as control surface (Ti-control) and then sandblasted with large-grit corundum and acid etched (SLA). Further chemical modifications were conducted using alkali and heat treatment (ASLA) and hydrogen peroxide and heat treatment (HSLA) alternatively. The surface properties were characterized by scanning electron microscopy (SEM), x-ray photoelectron spectroscopy (XPS), and contact angle and roughness measurements. Further evaluation of surface bioactivity was conducted by MC3T3-E1 cell attachment, proliferation, morphology, alkaline phosphatase (ALP) activity and calcium deposition on the sample surfaces. After insertion in the beagle's mandibula for a specific period, cylindrical implant samples underwent micro-CT examination and then histological examination. It was found that ASLA and HSLA surfaces significantly increased the surface wettability and MC3T3-E1 cell attachment percentage, ALP activity and the quality of calcium deposition in comparison with simple SLA and Ti-control surfaces. Animal studies showed good osseointegration of ASLA and HSLA surfaces with host bone. In conclusion, ASLA and HSLA surfaces enhanced the bioactivity of the traditional SLA surface by integrating the advantages of surface topography, composition and wettability.

1. Introduction

The clinical goal of dental implant surgery is the achievement of osseointegration, which is defined as the direct connection between implant and living bone without any soft tissue component interference. The higher the degree of osseointegration, the higher the mechanical stability and

the successful probability of implants are. Rapid and firm establishment of osseointegration has been considered as a persistent challenge for dental implants usually made of titanium [1–3]. Altering the surface properties of titanium implants, such as surface topography, composition and energy, has been seen as a method for hastening the bone healing process in order to get early osseointegration and subsequent clinical success [4, 5].

⁴ Author to whom any correspondence should be addressed.

Various methods were used to produce bioactive titanium surfaces including the physical method and the chemical method or their combinations to modify the implant surface [2, 3]. Alkali and heat treatments could create a hydrophilic and good bioactive surface which had nano-structured surface topography with an average pore size of 150–200 nm [5–7]. Lee *et al* reported that the improvement of bone reaction on the alkali- and heat-treated titanium implant was attributed to the nano-structured sodium titanate ($\text{Na}_2\text{Ti}_5\text{O}_{11}$ or $\text{Na}_2\text{Ti}_6\text{O}_{13}$) composition of the implant surface [7]. The sodium removal treatment was shown to be effective in improving the early bone–implant interface resistance to shear force [9]. The enhancement of bioactivity of titanium and its alloy by $\text{H}_2\text{O}_2/\text{HCl}$ and heat treatment was considered to be one of the potential surface modification techniques to improve the bioactivity of the titanium implants and was studied both *in vitro* and *in vivo* [10–12]. The minimum thickness of the titania gel layer and the optimal temperature of heat treatment were about 0.2 μm and 400–500 °C, respectively [11]. Yang *et al* demonstrated that SLA surface plus $\text{H}_2\text{O}_2/\text{HCl}$ and heat treatment can enhance peri-implant bone formation better than the SLA surface of Ti-6Al-4V [10].

The SLA titanium surface is a popular surface, which has been successfully applied in clinic for many years [13, 14]. However, dental implant therapy desires earlier loading and better osseointegration. In the present study, titanium surfaces having combined advantages of roughness, high surface energy and nano-structured properties together were designed by further treating the SLA surface with alkali or hydrogen peroxide and heat treatments in order to enhance the surface bioactivity and osseointegration process. The MC3T3-E1 cells were used to evaluate osteoblast behavior on the designed titanium surfaces. The effects of bone–implant integrations were examined by micro-CT analysis and histological observation for implant samples inserted in the beagle's mandibula.

2. Materials and method

2.1. Surface preparation

Commercially pure titanium (grade 2) disks with 15 mm diameter and 1.5 mm thickness were polished with 800# silicon carbide sand paper as a control surface (Ti-control). Some of them were sandblasted with large-grit corundum (200–500 μm) and then acid etched in 67% $\text{HCl}/\text{H}_2\text{SO}_4$ (1:1) at 80 °C for 10 min to get the well-known SLA surface. Subsequently, SLA surfaces were processed with two further chemical modification methods alternatively: alkali and heat treatment SLA surface (ASLA) and $\text{H}_2\text{O}_2/\text{HCl}$ and heat treatment (HSLA). ASLA was treated with 5 M NaOH at 150 °C in an autoclave for 4 h and then immersed in deionized water at 40 °C for 24 h before heat treatment at 600 °C for 1 h. HSLA was processed in 30% H_2O_2 and 0.1 M HCl solution at 80 °C for 20 min and successively heat treated at 400 °C for 1 h. The disks were cleaned with 15 min sonication cycles in acetone, ethanol and deionized water and then sterilized with 75% ethanol and rinsed with phosphate buffer saline solution (PBS) three times before cell culture and implantation.

2.2. Surface characterization

The surface topography was characterized using a scanning electron microscope (ESEM, AMRAY 1-1910FE). The secondary electron mode with an acceleration voltage of 15 kV was selected for SEM observation under high vacuum conditions. The surface chemical compositions were characterized using x-ray photoelectron spectroscopy (XPS, AXIS Ultra, UK) with monochromatic Al $K\alpha$ (1486.7 eV) radiation (15 mA, 15 kV) and low energy electron flooding for charge compensation. To compensate for the surface charging effects, binding energies were calibrated using the C1s hydrocarbon peak at 284.8 eV. The binding energies and atom concentration ratios were determined using the curve fitting by the CasaXPS software package.

The surface wettability was tested by contact angle (Dataphysics Instrument, Germany) in triple for each sample. Briefly, a 2 μl droplet of pure water was suspended from the tip of the microliter syringe supported above the sample stage. The image of the droplet was captured and the contact angle was measured using the OCA20 drop shape analysis program (Dataphysics Instrument, Germany). The surface roughness was measured with optical interferometry (Veeco, Dektak8, USA). Three specimens were selected and measured along two lines with 4 mm length respectively, carrying out six measurements for each group. The parameters of surface roughness were presented as the arithmetic average of height deviation in this study.

2.3. Cell–surface interactions

Osteoblast-like cell line MC3T3-E1 Subclone 4 (CRL2593, ATCC, USA) was cultured in α -MEM medium (Invitrogen) supplemented with 10% of fetal calf serum (FBS), 100 $\mu\text{g ml}^{-1}$ penicillin and 100 $\mu\text{g ml}^{-1}$ streptomycin in a humidified atmosphere with 5% CO_2 at 37 °C. After cell counting, MC3T3-E1 cells were seeded and cultured on all sample surfaces in 24-well culture plates at a density of 10^4 cells cm^{-2} for cell morphology, proliferation, differentiation and mineralization assays. The culture medium was refreshed every 2 days. Each experiment was performed in triple for each group and repeated twice to get similar results at least.

The initial attachment of cells was evaluated by measuring the quantity of the cells attached to titanium substrates at a high seeding density of 10^5 cells/well. After 20, 40, 60 and 120 min of incubation, the cells were rinsed with PBS three times gently to remove unattached cells and then 1 ml fresh cell culture medium was added. The cell proliferation assay was performed at 1, 3, 7 and 11 days. The quantities of the cells were measured by the MTT-based colorimetry assay. The cells were incubated at 37 °C for 4 h with 100 μl MTT reagent added to the culture media. The amount of formazan product formed was dissolved by 5% SDS for 18 h and then the solution's absorbance was measured using an ELISA reader (Model 680, Bio-Rad) at 570 nm with a reference wavelength of 630 nm. After 3 and 7 days of culture, the medium was removed and washed with PBS and then the cells were fixed with 2.5% glutaraldehyde in PBS for 60 min at room

temperature. After dehydration in graded series of alcohols, the samples were sputter coated with gold in a precision etching coating system (Model 682, Gantan), and then the cell morphologies were investigated by SEM observation.

After 24 h of cell seeding, the culture medium was changed to complete α -MEM medium containing 50 $\mu\text{g ml}^{-1}$ ascorbic acid and 10 mM disodium β -glycerophosphate (Amresco). After 7, 15 and 21 days of cultivation, the culture medium was removed and then 900 $\mu\text{l/well}$ 10 mM *p*-nitrophenylphosphate (Amresco) containing 2 mM MgCl_2 in a carbonate buffer solution (pH = 10.2) was added. After incubating at 37 °C for 60 min, 100 $\mu\text{l/well}$ of 1 M NaOH was added to stop the reaction. The ALP activity was evaluated as the amount of *p*-nitrophenol (PNP) released through the enzymatic reaction and measured at a 405 nm wavelength using an ELISA reader. For normalization, the total protein content was measured using a bicinchoninic acid assay kit (Sigma). Thus, the ALP activity was expressed in nmol of PNP produced per minute per mg protein. The mineralization capability of the cultured MC3T3-E1 cells was examined by calcium colorimetry-based assays after 7, 15 and 21 days under the same conditions as the ALP assay. For colorimetric detection of calcium deposition, the culture medium was washed with PBS and incubated overnight in 1 ml of 0.5 M HCl solution with gentle shaking. The solution was mixed with *o*-cresolphthalein complexone (Sigma) in alkaline medium to produce a red calcium–cresolphthalein complexone complex. The color intensity was measured by an ELISA reader at 570 nm wavelength absorbance.

2.4. Animal studies

Six adolescent beagle dogs were used for animal studies. Cylindrical titanium implant specimens with diameter 3 mm and length 5 mm were prepared with different surface treatment methods according to section 2.1. The implantation sites having diameter of 3 mm were prepared by drilling into the flat surfaces of the mandible. Figure 5(a) shows the insertion position for specimens with different surface properties at one side of the mandible. Finally, surgical sites were sutured with suture thread. The Peking University Animal Research Committee approved this protocol and all experiments were performed in accordance with the standard of Beijing Association on Laboratory Animal Care. The beagles were set for euthanasia and the mandible containing cylindrical implants were retrieved after 1 and 3 months of implantation and then stored in 10% buffered formalin before following evaluations.

Specimens with titanium implants and the surrounding bone tissue were scanned with a commercially available desktop microCT scanner (Skyscan 1076, Aartselaar, Belgium). This system was set at a resolution of 18 μm for all the samples at 100 kV, 80 μA and a 360° rotation with the step of 0.4°, with a 0.5 mm thick aluminum filter to optimize the contrast. Three-dimensional reconstruction and peri-implant bone volume percentage were analyzed using Skyscan™ CT-analyzer software. Three-dimensional reconstruction of bone architecture analysis was performed in

the peri-implant cancellous bone region and the cortical bone region, respectively. Peri-implant bone volume/tissue volume (BV/TV) at the cancellous bone region and the cortical bone region were calculated at the same threshold of gray value from microCT images, respectively. After microCT examination, the specimens were dehydrated in an ascending series of alcohol rinses and embedded in a light-curing epoxy resin without decalcification. The embedded specimens were sawed along the longitudinal axis of the cylindrical implants. The specimens were ground to a thickness of 30 μm with a grinding system (Exakt Apparatebau, Norderstedt, Germany). The sections of the specimens were stained with methylene blue, and observed under a light microscope at 100× magnification.

2.5. Statistical analysis

Six mutually independent measurements were obtained for all cell and animal assays. Each experimental result is expressed as mean \pm standard deviation (SD). The significance of the obtained data was calculated using one-way ANOVA, followed by Tukey's test for a multiple comparison procedure with a confidence level of 95% ($p < 0.05$) considered statistically significant and 99% ($p < 0.01$) considered very significant.

3. Results

3.1. Surface characterizations

The surface topographies of Ti-control, SLA, ASLA and HSLA are shown in figures 1(a)–(d) by SEM observation. At low magnification, micro rough surface of the SLA, ASLA and HSLA were readily observed compared with the smooth Ti-control surface with slit scratch because of mechanical polishing. SLA surface topography showed macro and micro pits which were similar to previous reports [13, 14]. Residual corundum particles were not found on the surfaces after acid etching and cleaning. Some cracks could be found on the ASLA surface because of the heat treatment process. The inset pictures with high magnification showed nanofiber-like features of the ASLA surface which were similar to the report of Wang *et al* [8]. Nanopore-like topographic characterization could be seen at high magnification of the HSLA surface which had a similar topography to the SLA surface at low magnification.

The surface compositions of the different samples are shown in figure 2 and table 1 by XPS analysis. The major elements on all surfaces were titanium, carbon, oxygen and nitrogen. The ASLA surface contained Na element which might due to sodium titanate formed by alkali and heat treatment. These surfaces were oxidized and polluted by carbon contaminants; however ASLA and HSLA surfaces had less carbon ratio than that of Ti-control and SLA surfaces. Surface roughness and contact angle are listed in table 1 The Ti-control surface had the lowest roughness, while the SLA surface had the highest roughness. The ASLA and HSLA had slightly lower roughness than that of the SLA surface because of the further modification. As surface modification affected surface wettability, the ASLA and HSLA surfaces had super hydrophilic properties with a water contact angle less than

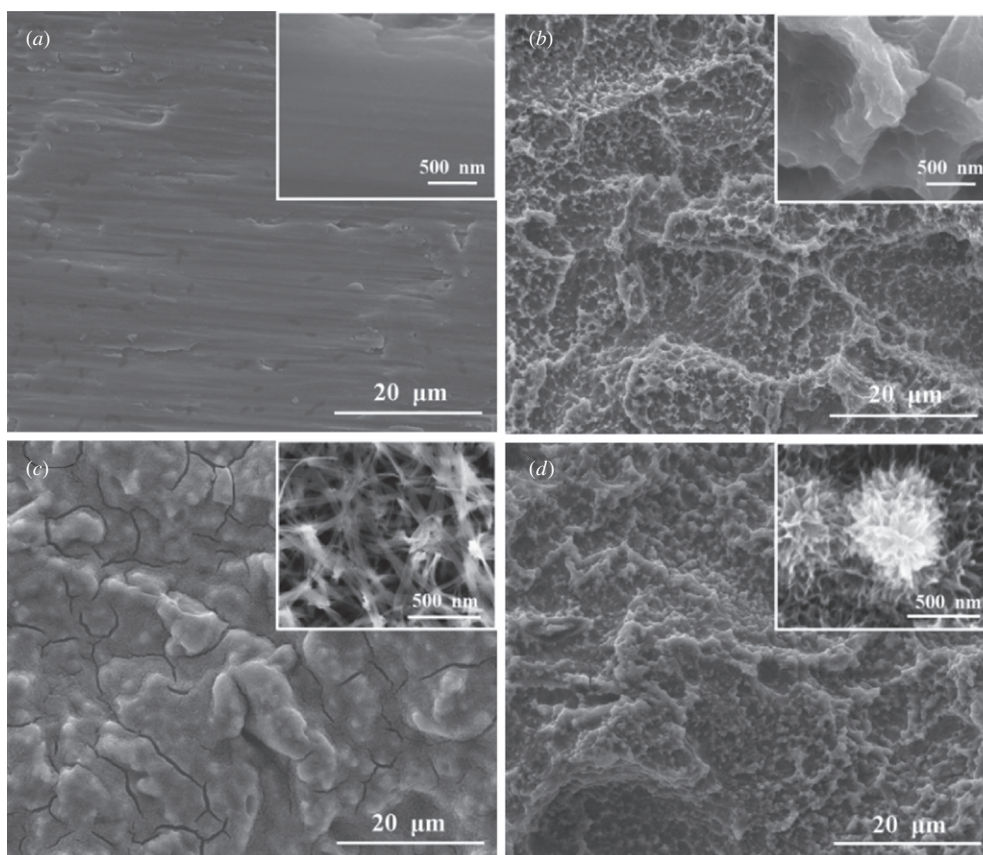


Figure 1. SEM images showing surface topography of (a) Ti-control, (b) SLA, (c) ASLA and (d) HSLA. The inset pictures with high magnification for observation of nanoscale topography.

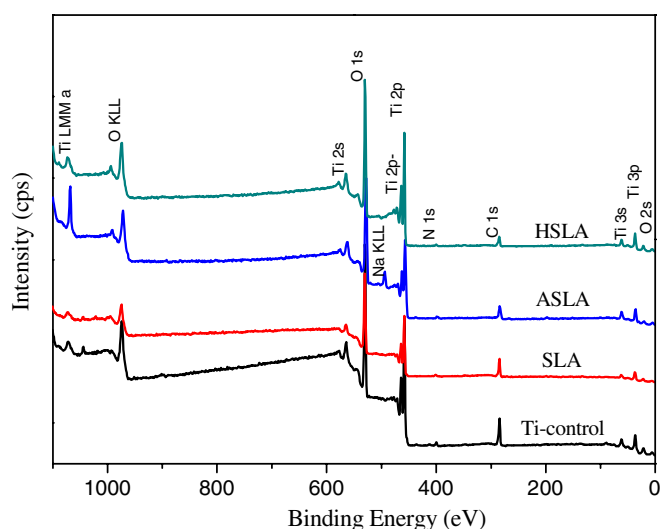


Figure 2. XPS spectra of Ti-control, SLA, ALSA and HSLA surfaces.

5°. The SLA surface presented the most hydrophobic surface property.

3.2. Cell–surface interactions

The cell attachment and proliferation results were expressed as the number of cells normalized to that of the control surface

after expected time cultured on sample surfaces. After 20, 40, 60 and 120 min incubation, the number of MC3T3-E1 cells attached on ASLA and HSLA surfaces was greater than that on SLA and Ti-control surfaces especially at the time points of 40 and 60 min (figure 3(a)). The cell proliferation results indicated that all surfaces had good cytocompatibility with the proliferation ratio near to or greater than the Ti-control group at all testing time points. The HSLA surface had a significantly higher proliferation ratio than that of the SLA surface at 3 and 7 days. Thus, ASLA and HSLA surfaces increased the cell attachment and proliferation ratio at early stage.

MC3T3-E1 cells on SLA, ASLA and HSLA surfaces were more extending with numerous cytoplasmic extensions and filopodia than that on the Ti-control surface at 3 days of culture, as shown in figure 4. Cells reached over 100% confluence at 7 days for all sample surfaces. Figure 3(c) demonstrates that the ALP activity of MC3T3-E1 cells increased from the beginning on all sample surfaces. The ALP activity of MC3T3-E1 cells on ASLA and HSLA surfaces was significantly higher than that of SLA and Ti-control groups. The ASLA surface seemed to have the best ability to enhance ALP products which would result in phenotypes of osteoblast as well as the quantity of calcium deposition, as figure shown in 3(d).

Table 1. Surface composition, roughness and contact angle for various samples.

| | Ti-control | SLA | ASLA | HSLA |
|-------------------------------------|-----------------|-----------------|-----------------|-----------------|
| Element Ti (at.%) | 20.90 | 17.17 | 25.03 | 25.89 |
| Element O (at.%) | 50.69 | 47.13 | 54.10 | 57.84 |
| Element C (at.%) | 26.33 | 33.20 | 18.18 | 14.30 |
| Element N (at.%) | 1.56 | 2.13 | 1.01 | 1.27 |
| Element Na (at.%) | – | – | 1.36 | – |
| Average roughness (μm) | 0.28 ± 0.05 | 2.85 ± 0.26 | 2.63 ± 0.20 | 2.50 ± 0.23 |
| Contact angle (degree) | 59.4 ± 2.89 | 81.5 ± 5.83 | <5 | <5 |

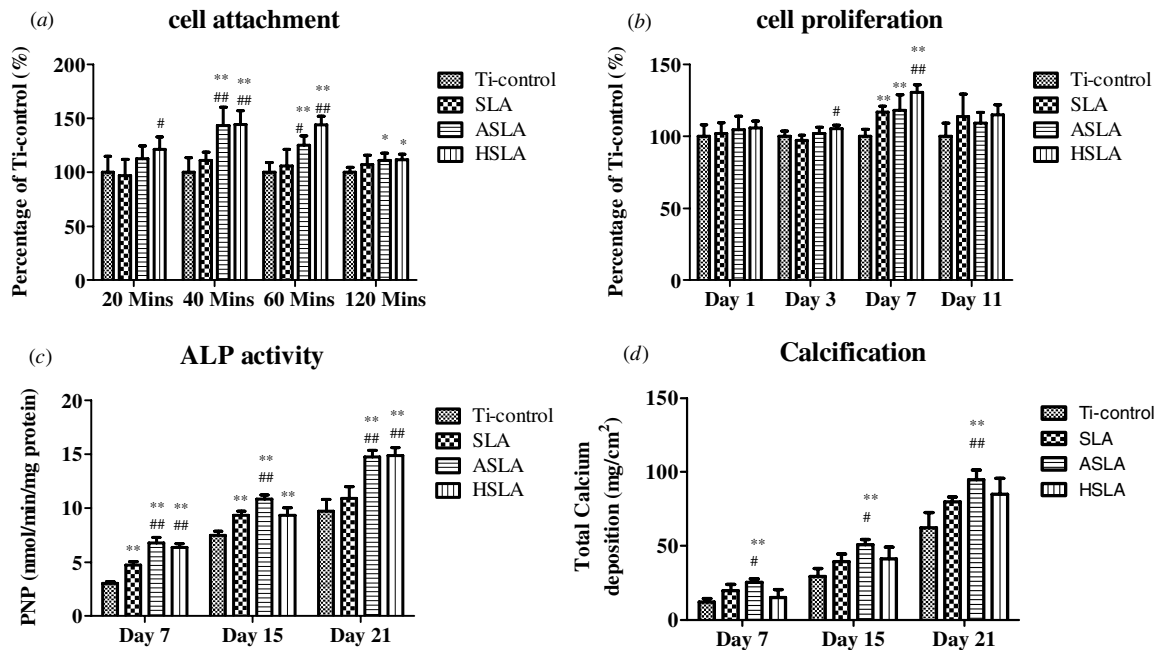


Figure 3. (a) MC3T3-E1 cell attachment percentage on different surfaces. (b) MC3T3-E1 cell proliferation ratio on different surfaces. (c) ALP activity normalized to the protein content of osteoblastic cells cultured on the titanium surfaces. (d) Calcium deposition quantity on surfaces. Symbols * and ** mean a significant difference in comparison with the Ti-control group $P < 0.05$ and $P < 0.01$, respectively. Symbols # and ## mean a significant difference in comparison with the SLA group $P < 0.05$ and $P < 0.01$, respectively.

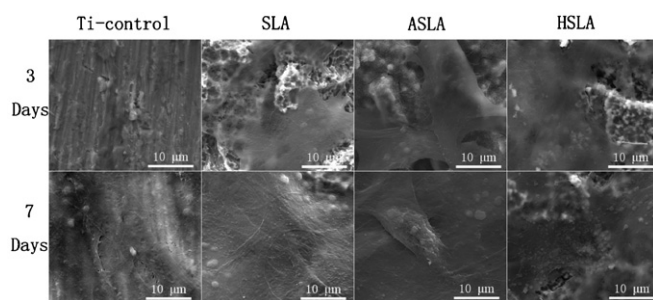


Figure 4. Morphologies of MC3T3-E1 cells after 3 and 7 days cultured on Ti-control, SLA, ASLA and HSLA surfaces.

3.3. Animal studies

MicroCT analysis presented that implants and bone could reach good osseointegration after 1 and 3 months of implantation. Figures 5(b), (c) show the representative x-ray images of the beagle’s mandibula integrated with implant samples. The three-dimensional architecture of integrated bone with implant samples were shown as segments with height 2.5 mm and diameters 4.5 mm in figures 5(d) and (f).

The three-dimensional architecture of peri-implant cancellous bone showed porous structure. Higher cancellous BV/TV could be found around the ASLA and HSLA surfaces, in comparison to that of Ti-control (figure 5(e)). The cortical bone of peri-implant had dense feature (figure 5(f)) with BV/TV over 90% after 3 month healing. Compared with the SLA surface, there was no statistical significant difference for BV/TV in both cancellous bone and cortical bone.

The histological examinations presented that new bone could be found around implants as the bright red region shown in figure 6. No significantly greater percentage of bone–implant contact was observed adjacent to ASLA and HSLA surfaces compared with that around SLA and Ti-control surfaces. MicroCT examination and histological observation demonstrated that bone could integrate with all surfaces well but there were no significant differences for ASLA and HSLA surfaces compared with the SLA surface.

4. Discussion

All surfaces showed good biocompatibility with both cell responses and animal studies. Hydrophilic ASLA and

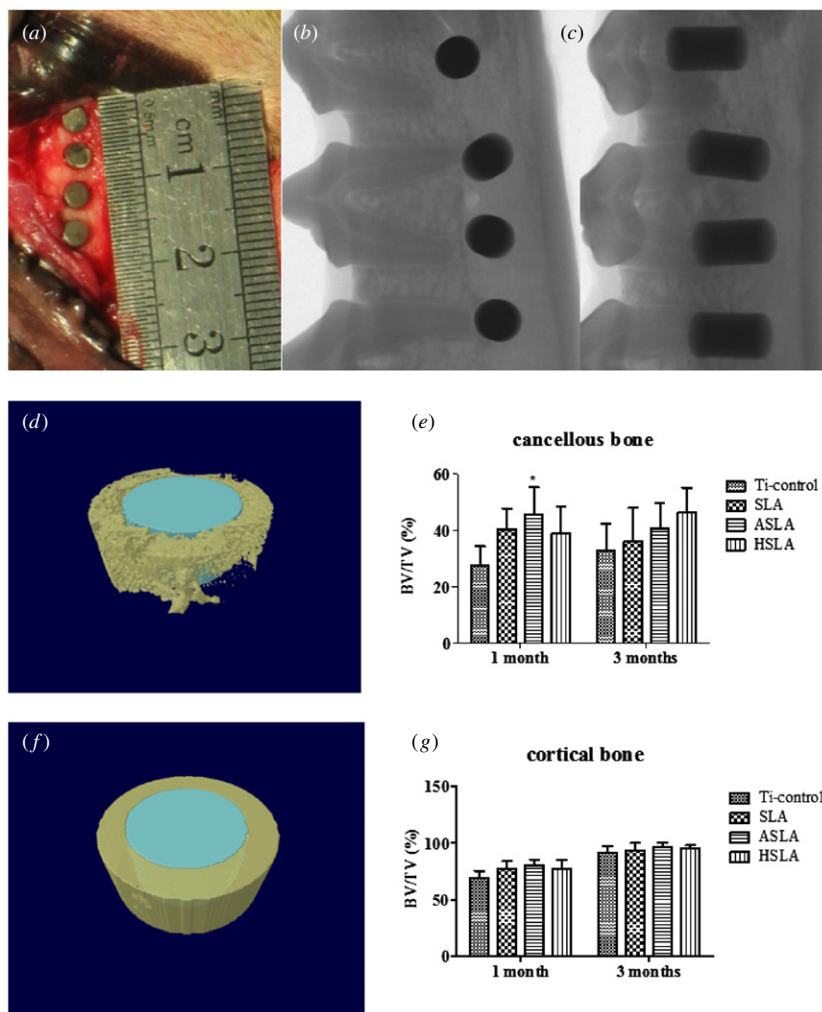


Figure 5. Implantation of four specimens in one side of beagle’s mandibula (a). Representative x-ray images for four samples in mandibula after 3 month implantation (b, c). Representative three-dimensional reconstruction (d) of bone architecture in cancellous bone (f) and cortical bone (f) integrated around implant shown as segments with height of 2.5 mm and thickness of 0.75 mm peri-implant bone. Peri-implant bone volume/tissue volume (BV/TV) at cancellous bone region (e) and cortical bone region (g).

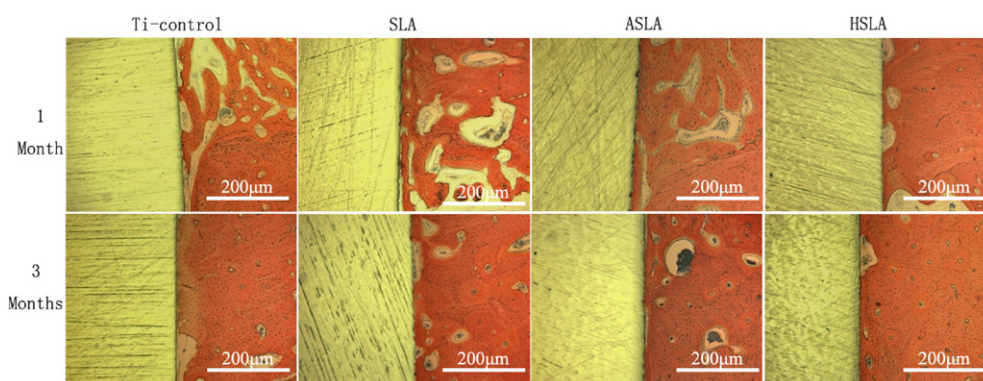


Figure 6. Representative histological images stained by methylene blue after the implantation period of 1 month and 3 months for Ti-control, SLA, ASLA and HSLA surfaces.

HSLA surfaces with micro- and nano-structured surface topographies provided a favorable surface for cell attachment and proliferation. In the case of the ASLA surface, ALP activity and calcium deposition quality were found to be higher for every time point than that of the SLA surface. ASLA

and HSLA surfaces improved cellular and bone responses and might benefit osseointegration and dental implant therapy.

It is not only the microscale alteration such as mechanical interlocking but also the nanoscale alteration that can enhance the adhesion ability and phenotypes of osteoblast, and

subsequently bone anchoring and biomechanical stability of implants in host bone [15]. Nano-structured materials could improve the cell adhesion and tissue biocompatible responses and result in better osseointegration [16, 17]. Nano-structured surface features could decrease the activation energy barrier and reduce the interfacial energy between bone formative soft tissue and mineralized bone [18]. ASLA and HSLA altered not only the surface topography but also the chemical composition of the surface. The micro- and nano-structured sodium titanate layer (ASLA) and titanium dioxide layer (HSLA) may be beneficial for the fast nucleation on the surfaces during the bone mineralization period. The ASLA and HSLA surfaces with much lower carbon contamination than that of SLA and Ti-control surfaces accorded with the fact that the reduction of carbon contamination were considered to be a reason of enhancement of titanium surface bioactivity [19, 20]. Aita *et al* suggested that the contamination was with hydrocarbons which may affect the bioactivity of the Ti surface and could be reduced by ultraviolet irradiation [19]. The ASLA and HSLA may be other ways to reduce the surface contamination. Besides the surface topography and composition, the improvement of surface wettability of ASLA and HSLA surfaces may be another reason for better osteoblastic behavior and bone-implant integration. The hydrophilic SLA surfaces have been proved to gain better bioactivity than the hydrophobic SLA surface by the N₂ protection or ultraviolet irradiation [19–22]. High surface energy has been reported to be desirable for dental implants because increased wettability would enhance the interaction between the implant surface and its surrounding biological environment [21, 22]. These data suggested that surface topography, composition and wettability could be improved and work together to enhance the bioactivity of titanium surfaces.

5. Conclusions

Titanium surfaces having combined advantages of surface topography, composition and wettability together were prepared and characterized. Increased wettability of ASLA and HSLA surfaces with micro and nano-structured topography led to higher cell attachment, proliferation ratio, ALP activity and calcium deposition quantity than that of SLA and Ti-control surfaces for MC3T3-E1 cells. The HSLA surface may be favorable for cell proliferation and the ASLA surface may be favorable for osteoblast phenotypes. Animal studies presented that ASLA and HSLA surfaces had good osseointegration by micro-CT and histological examinations. Based on the *in vitro* and *in vivo* studies, ASLA and HSLA

surface modifications may be the promising methods to generate better bioactivity and osseointegration than that of the traditional SLA and smooth titanium surfaces.

Acknowledgments

This work was supported by the State Key Development Program for Basic Research of China (Grant 2007CB936103), Peking University Interdisciplinary and Emerging Disciplines Research Foundation (grant PKUJC2009001), Beijing Municipal Natural Science Foundation (2082010) and Peking University's 985 Grant.

References

- [1] Geetha M, Singh A K, Asokamani R and Gogia A K 2009 *Prog. Mater. Sci.* **54** 397–425
- [2] Schliephake H and Scharnweber D 2008 *J. Mater. Chem.* **18** 2404–14
- [3] Stanford C M 2008 *Aust. Dent. J.* **53** S26–S33
- [4] Ismail F S M, Rohanizadeh R and Atwa S 2007 *J Mater Sci. Mater. Med.* **18** 705–14
- [5] Coelho P G, Granjeiro J M and Romanos G E 2009 *J. Biomed. Mater. Res. B* **88** 579–96
- [6] Kim H M, Miyaji F, Kokubo T and Nakamura T 1996 *J. Biomed. Mater. Res.* **32** 409–17
- [7] Lee B H, Kim Y D, Shin J H and Lee K H 2002 *J. Biomed. Mater. Res.* **61** 466–73
- [8] Wang X J, Li Y C, Lin J G, Yamada Y, Hodgson P D and Wen C E 2008 *Acta Biomater.* **4** 1530–5
- [9] Fawzy A S and Amer M A 2009 *Dent. Mater.* **25** 48–57
- [10] Yang G L, He F M, Zhao S S, Wang X X and Zhao S F 2008 *Int. J. Oral Maxillofac. Implants* **23** 1020–8 (<http://www.ncbi.nlm.nih.gov/pubmed/19216270>)
- [11] Wang X X, Hayakawa S, Tsuru K and Osaka A 2002 *Biomaterials* **23** 1353–7
- [12] Wang X X and Osaka A 2001 *Mater. Sci. Forum* **394–395** 165–8
- [13] Lohmann C H *et al* 2002 *J. Biomed. Mater. Res.* **62** 204–13
- [14] Cochran D L, Schenk R K, Lussi A, Higginbottom F L and Buser D 1998 *J. Biomed. Mater. Res.* **40** 1–11
- [15] Lauer G, Wiedmann-Al-Ahmad M, Otten J E, Hubner U, Schmelzeisen R and Schilli W 2001 *Biomaterials* **22** 2799–809
- [16] Mendonca G, Mendonca D B S, Aragao F J L and Cooper L F 2008 *Biomaterials* **29** 3822–35
- [17] Kripparamanan R, Aswath P, Zhou A, Tang L P and Nguyen K T 2006 *J. Nanosci. Nanotechnol.* **6** 1905–19
- [18] Lee B H, Lee C, Kim D G, Choi K, Lee K H and Do Kim Y 2008 *Mater. Sci. Eng. C* **28** 1448–61
- [19] Aita H *et al* 2009 *Biomaterials* **30** 1015–25
- [20] Buser D *et al* 2004 *J. Dent. Res.* **83** 529–33
- [21] Zhao G *et al* 2005 *J Biomed. Mater. Res. A* **74** 49–58
- [22] Lim J Y, Shaughnessy M C, Zhou Z Y, Noh H and Vogler E A 2008 *Biomaterials* **29** 1776–84